

## Research Article

# Development of a High-Performance Magnetic Field Sensor and Its Application to a Magnetic Field Visualization System Using the Augmented Reality Technique

Hisahide Nakamura <sup>1</sup>, Yukio Mizuno,<sup>2</sup> and Shrinathan Esakimuthu Pandarakone<sup>2</sup>

<sup>1</sup>Research and Development Division, TOENEC Corp., Nagoya 457-0819, Japan

<sup>2</sup>Department of Electrical and Mechanical Engineering, Nagoya Institute of Technology, Nagoya 466-8555, Japan

Correspondence should be addressed to Hisahide Nakamura; hisahide-nakamura@toenec.co.jp

Received 17 May 2019; Revised 23 July 2019; Accepted 30 July 2019; Published 9 September 2019

Guest Editor: Dongfeng He

Copyright © 2019 Hisahide Nakamura et al. This is an open access article distributed under the Creative Commons Attribution License, which permits unrestricted use, distribution, and reproduction in any medium, provided the original work is properly cited.

Two- or three-dimensional visualization of magnetic flux density distribution around sources is quite informative for understanding the field environment intuitively. Measurement of magnetic flux density, as well as positioning of measuring points in space, has to be performed in a short time because temporal variation in the source current results in different field environments. It is also valuable to obtain the frequency spectrum of the magnetic field simultaneously at the time of field measurement, especially for sources generating high-frequency components like inverter-driven equipment. This paper develops a high-performance magnetic field sensor which satisfies the above requirements. And, as an application of it, the magnetic field visualization system using the augmented reality (AR) technique is proposed by combining two sensors: one is a magnetic field sensor described above, and the other is a Kinect sensor which has a skeleton tracking function as position determination.

## 1. Introduction

Visualization of the magnetic field is an effective measure to understand the field environment intuitively. Some papers treated this topic. For example, an interactive visualization system for fast and easy perception of electromagnetic force and electromagnetic field distribution [1], a real-time visualization system which can provide the drawing of the magnetic field generated by a bar magnet and ferromagnetic material [2], and interactive visualization of electromagnetics for engineering education programs [3] have been proposed.

Quantification of the magnetic field has been made by spot measurements around household appliances [4–6] and power facilities [7–11]. Magnetic flux density and/or its frequency characteristics at measuring points have been reported in these researches, but planar or spatial distribution of magnetic flux density around sources has been

scarcely evaluated. One of the reasons is that it is a time-consuming and tedious work to carry out spot measurement many times at various points in space. Another reason is that a short-time measurement is required in some cases because magnetic field distribution is bound to change due to temporal variation of current flowing in sources.

The authors proposed a novel system using Kinect to visualize the magnetic field environment around sources and its effectiveness was confirmed by performing some experiments in the laboratory [12]. The system is unique and promising because spot measurements in space of interest can be carried out in a considerably short time compared with conventional measuring procedures and visualization of field distribution can be achieved. The sensor has a disadvantage that the frequency range is below 1 kHz. In case of the measurement of the magnetic flux density generated from electrical equipment driven by commercial frequency,

this range is acceptable. However, it is unavailable for the measurement of the magnetic flux density generated by inverter-driven electrical equipment.

Some meters are available for measurement of magnetic flux density up to 400 kHz [13, 14]. In these meters, magnetic flux density can be obtained but its frequency spectrum is unavailable. Data have to be recorded in a PC with the dedicated software after transferring them from meters to a PC via a cable. The dimensions of the sensor probe are rather large, which is suitable to obtained magnetic field characteristics around power equipment. The field environment generated by a small source like a household appliance is not necessarily evaluated satisfactorily.

In order to understand the magnetic field environment around household appliances in detail and to propose the new visualization system, in this paper, first, a high-performance magnetic field sensor is developed. The frequency range of the sensor is from 30 Hz to 400 kHz. And this sensor can indicate both the resultant magnetic flux density and its frequency components simultaneously. This sensor enables to store data in an external PC by transferring them with Wi-Fi as well as in a USB memory inserted to the USB port on the front of the detector. Next, as an application of this magnetic field sensor, a magnetic flux density visualization system is developed by using the AR technique. AR is a technology for achieving a more realistic expression, which enables adding information created by a computer on an actual scenery, landscape, etc. This visualization system with the AR technique is realized by combining the developed magnetic field sensor and the Kinect sensor, which has the tracking function. Finally, the usefulness of the visualization system based on the AR technique is verified through some experiments.

## 2. Development of a Magnetic Field Sensor

*2.1. Structure of Specification of the Magnetic Field Sensor.* The appearance of the developed magnetic field sensor is shown in Figure 1. This sensor consists of three parts: a detector, a probe, and a switch to trigger measurement. The size of the detector's body is 210(W) × 230(D) × 90(H) mm and the weight including the probe is 2150 g.

The frequency range is from 30 Hz to 400 kHz and the measurement range of the sensor is set from 0.2 to 200  $\mu$ T. The error of the sensor is designed to be less than 2% and it is confirmed by calibration using a Helmholtz coil.

In the detector, a Raspberry Pi [15] is adopted as a processing computer. The Raspberry Pi is a kind of computer. Though it is very small, various functions and some ports, such as a USB and Ethernet, are equipped. An operating clock of Raspberry Pi is from 900 MHz to 1 GHz, while that of a microcomputer is several 10 MHz. Thus, the Raspberry Pi can perform high-speed calculation compared with the microcomputer in signal processing and processing of the input and output of data.

The power of the sensor is supplied from AC100V or a portable battery for cell phones. Since this detector's body weight is about 2 kg, it can be used as a portable sensor with the battery.

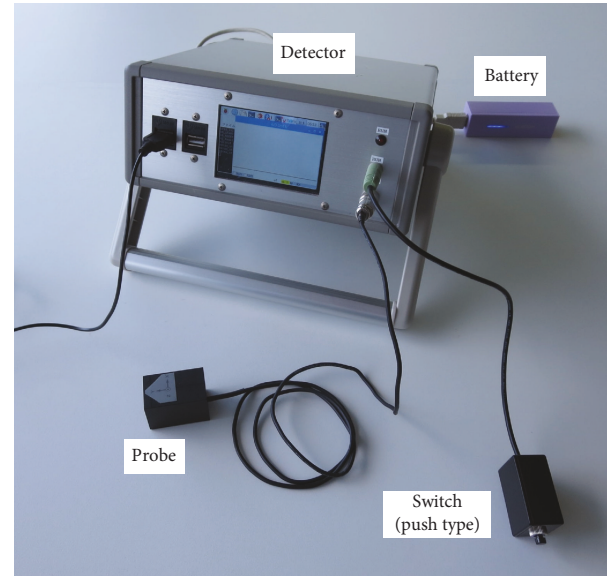


FIGURE 1: Magnetic field sensor.

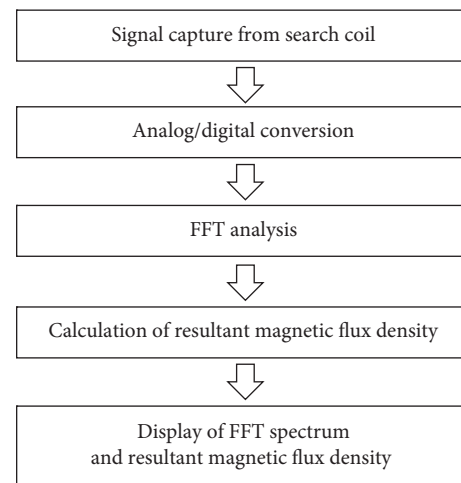


FIGURE 2: Flow of signal processing of the magnetic field sensor.

Commencement of measurement is triggered by the switch. Two types of switch are prepared: one is a push switch and the other is a toggle switch. The push switch is for one-shot operation, and the toggle switch is for long-time, continuous operation. A user easily selects the switch according to a purpose.

*2.2. Signal Processing.* The flow of the signal processing of the magnetic field sensor is shown in Figure 2. First, the signal of the magnetic flux density is detected by the probe. It is converted to a digital signal through an A-D converter and is taken in the Raspberry Pi. Raspberry Pi can use a free software: PYTHON. PYTHON is a programming language which has become popular recently in the field of computational science; it has characters that make programming easier and a smaller number of lines than programming language C. In this sensor, the FFT analysis is available with PYTHON. Not only the resultant magnetic flux density but

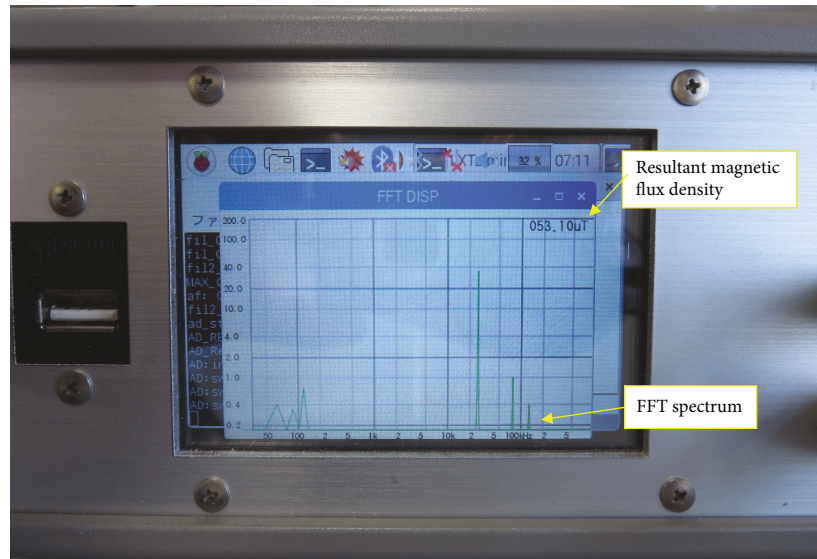


FIGURE 3: Example of the display.

also its frequency spectrum can be calculated. Finally, both the frequency spectrum and the value of the resultant magnetic flux density are displayed on the LCD of the detector, as shown in Figure 3. In the display of the FFT spectrum, a common logarithm is used in the scale of the horizontal and the vertical axes.

When a USB memory is inserted into the USB port in the front of the detector, Raspberry Pi recognizes it and measured data are saved automatically in a text form. When measurement is repeated, data can also be stored in a hard disk in an external PC by transferring them with Wi-Fi.

### 3. Visualization System

**3.1. Structure of the Visualization System.** As an application of the abovementioned magnetic field sensor, the visualization system of the magnetic field is proposed. The structure of the proposed visualization system is shown in Figure 4. It consists of three parts: the magnetic field sensor, a Kinect sensor, and a PC.

The magnetic flux density at various spots is measured by moving the probe. Then, the resultant magnetic flux density and its frequency components are calculated inside the magnetic field sensor. These data are combined into one file and the transmission packet is generated and stored in the specific folder in the Raspberry Pi. Once the PC confirms a file in the specific holder by wireless communication with the sensor, the file is sent to the PC automatically. FFT analysis in the sensor is one of features of the present system, which enables load reduction on the PC during image processing for visualization and indication of the result on a monitor in a short time.

For wireless data transmission between the magnetic field sensor and the PC, both Wi-Fi and Bluetooth are conceivable. Wi-Fi enables a faster communications, better range, and better wireless security than Bluetooth. To achieve the visualization system, a high data transfer rate is required. For this reason, Wi-Fi is adopted in this visualization system.

However, Wi-Fi standardly equipped in the Raspberry Pi cannot be used because data transmission is blocked by the detector's case body. In order to avoid this, an external Wi-Fi dongle is used by inserting into the USB port in the front surface of the magnetic field sensor.

**3.2. Kinect Sensor [16].** This visualization system of the magnetic field is realized by using a Kinect sensor. A Kinect sensor is one of the motion capture sensors and was released by Microsoft in 2011. It has both an RGB camera and a depth camera and is capable of obtaining information on both the human's skeleton position and the actual background image. Since a Kinect sensor has a function of skeleton tracking, the position of a human's skeleton can be identified continuously by following the movement of the human body. Furthermore, it is inexpensive; the Kinect sensor became familiar among many researchers to analyze the positioning in various fields [17, 18]. Kinect for Windows SDK is also provided as a software development kit. By using Kinect for Windows SDK and based on a depth information obtained from the depth sensor, the human target is extracted as an image. Also, three-dimensional coordinates of his/her 20 joints can be obtained and indicated in the image. Henceforth, both the Kinect for Windows and Kinect for Windows SDK are referred as a Kinect sensor.

The proposed visualization system uses the tracking function of a Kinect sensor. Three-dimensional positional coordinates of the hand are easily obtained. In this system, the position of each measurement point is determined by the position of the hand which holds the search coil.

**3.3. Data Processing by PC for Realization of the AR Visualization.** The proposed visualization system starts to measure the magnetic flux density after the skeleton tracking Kinect operates. The magnetic flux density at a given measuring point is displayed on a PC screen by various colors depending on its strength. This makes the visualization system based on the AR technique possible.

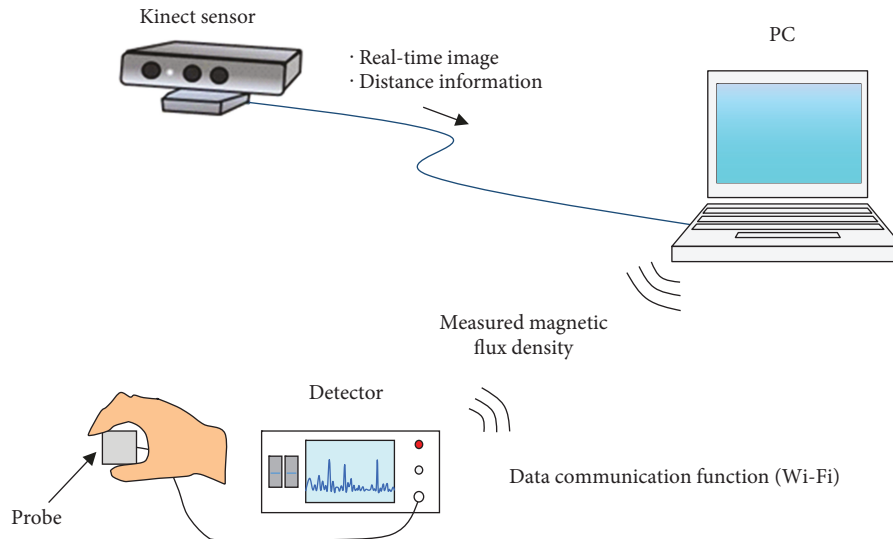


FIGURE 4: Structure of the visualization system.

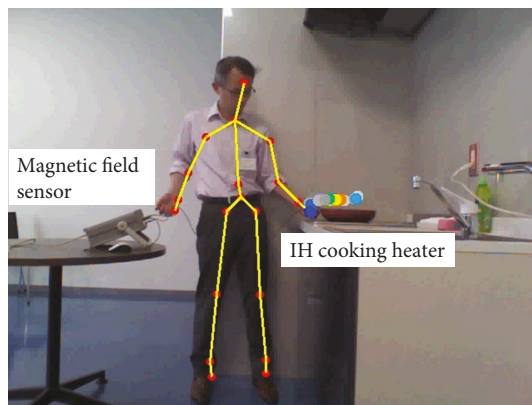


FIGURE 5: Visualization of the magnetic field of the area around the IH cooking heater.

When the maximum magnetic flux density to be measured is expected to be less than  $20 \mu\text{T}$ , gray and red marks are used to indicate 0 and  $20 \mu\text{T}$ , respectively. Blue, light-blue, green, yellow, and orange marks are allocated to magnetic flux densities between 0 and  $20 \mu\text{T}$ . In the case of indication of magnetic flux density of up to  $200 \mu\text{T}$ , a red mark is allocated to  $200 \mu\text{T}$  and other colors are used similarly to the case of  $20 \mu\text{T}$ . Additionally, gradation is introduced to display the measurement results. The system requires 8 sec for the data acquisition and the indication of a colored mark on the monitor screen.

#### 4. Visualization of Distribution of Magnetic Flux Density

*4.1. Visualization of the Distribution of the Magnetic Flux Density around IH Cooking Heater-1.* The usefulness of this visualization system is verified through some experiments. In this section, an IH cooking heater is selected as a target equipment. When water in a frying pan is being heated on this IH cooking heater, the magnetic flux density around

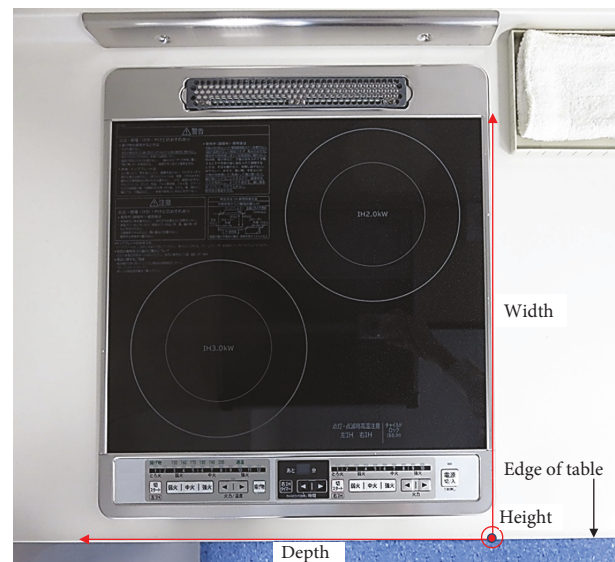


FIGURE 6: Setting of the coordinate system of IH cooking heater-1.

the cooking heater is visualized. The output of this IH cooking heater is 3.0 kW.

Visualization results of the magnetic flux density displayed on a PC are shown in Figure 5. In this figure, yellow lines and red circles on the body are skeletons and joints, respectively, recognized by Kinect. Magnetic flux density is shown by a color mark as described in Section 3.3; considering the maximum magnetic flux density obtained, red is allocated to  $20 \mu\text{T}$ . The operator holds the probe in his/her left hand and pushes the switch with the right hand. Though the magnetic field sensor is portable, it is put on the desk during this experiment. According to Figure 5, it can be easily realized that a high magnetic flux density is recorded in the area close to the coil of the IH cooking heater. In this way, by utilizing the latest AR technology actively, valuable information can be added to the actual image of a measuring site;

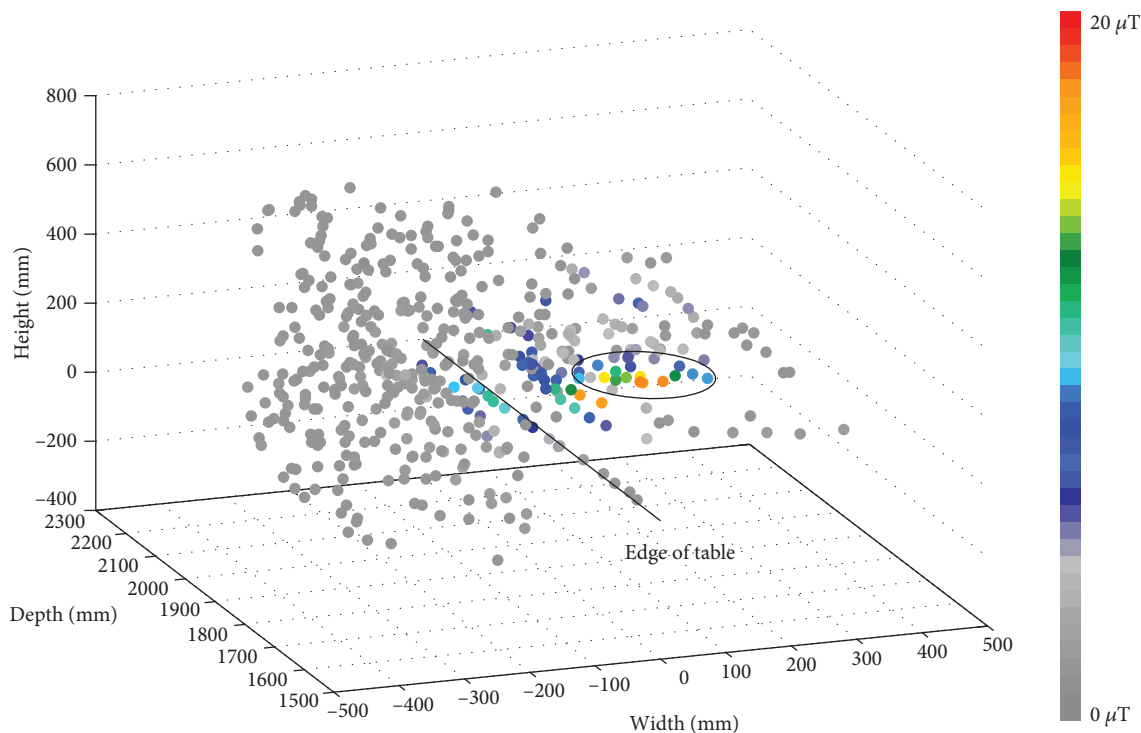


FIGURE 7: Three-dimensional distribution of magnetic flux density generated by IH cooking heater-1.

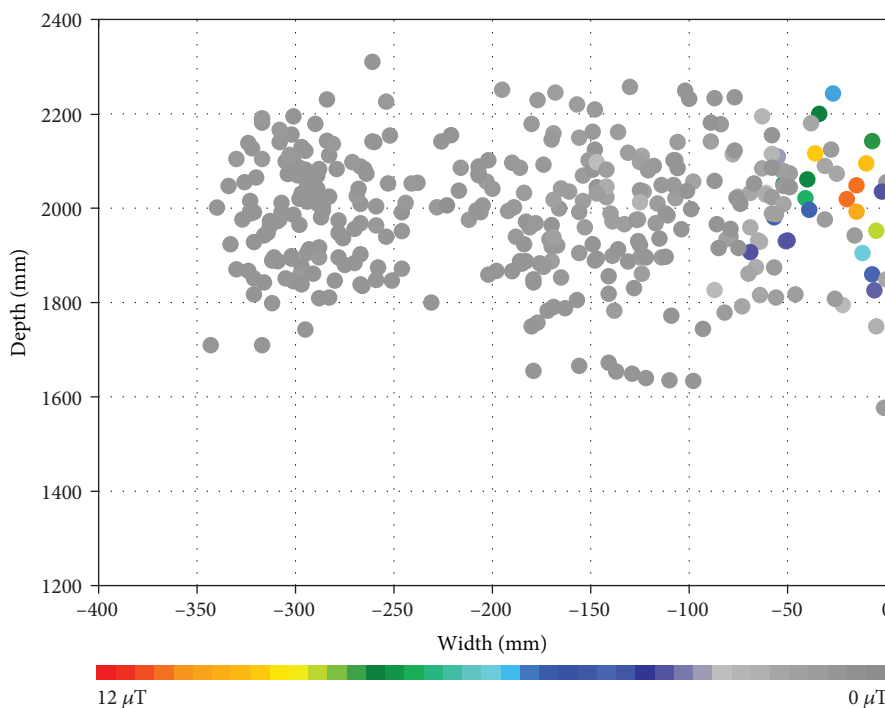


FIGURE 8: Two-dimensional distribution of magnetic flux density in the area where someone who cooks food stands (width-depth).

it becomes possible to visualize the invisible physical quantities like magnetic field flux density.

As mentioned above, this system can record both the magnetic flux density and the three-dimensional coordinates of the measurement points. The coordinate system is set as shown in Figure 6. “Width” is taken in the direction

of the distance from the front of the cooking table toward the back. “Width” is set to be zero at the front of the cooking table. “Height” is taken in the direction of the vertical axis. “Height” is set to be zero at the surface of the cooking table. “Depth” is set in the direction of the distance from the Kinect sensor.

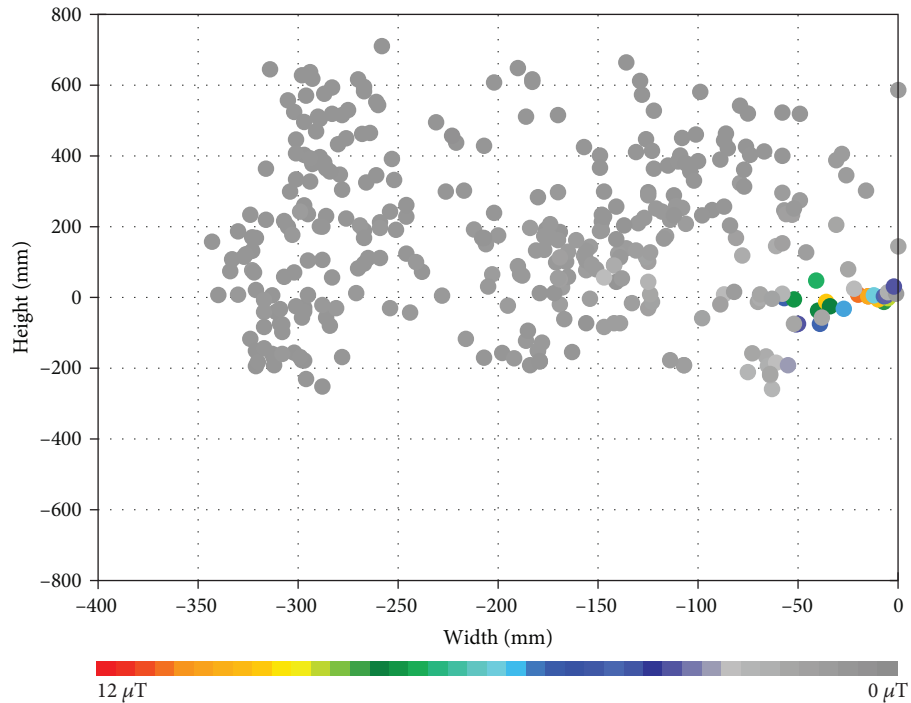


FIGURE 9: Two-dimensional distribution of magnetic flux density in the area where someone who cooks food stands (width-height).

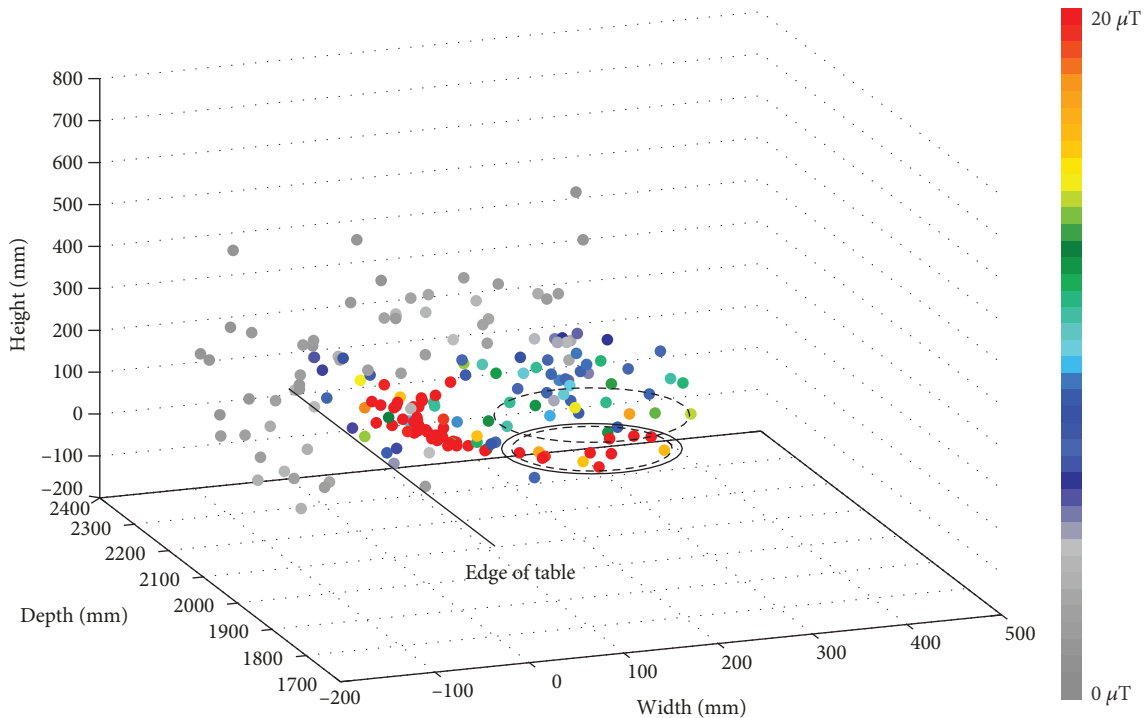


FIGURE 10: Three-dimensional distribution of magnetic flux density around IH cooking heater-2.

Figure 7 shows the three-dimensional distribution of the magnetic flux density around the IH cooking heater. Magnetic flux density at 492 measurement points is indicated. The circle in this figure means the position of the IH cooking heater. Figure 7 reveals that the magnetic flux den-

sity gets smaller as the measuring point leaves from the IH cooking heater.

Furthermore, two-dimensional distribution of the magnetic flux density is shown in Figures 8 and 9. These figures display the magnetic field density obtained in a half space

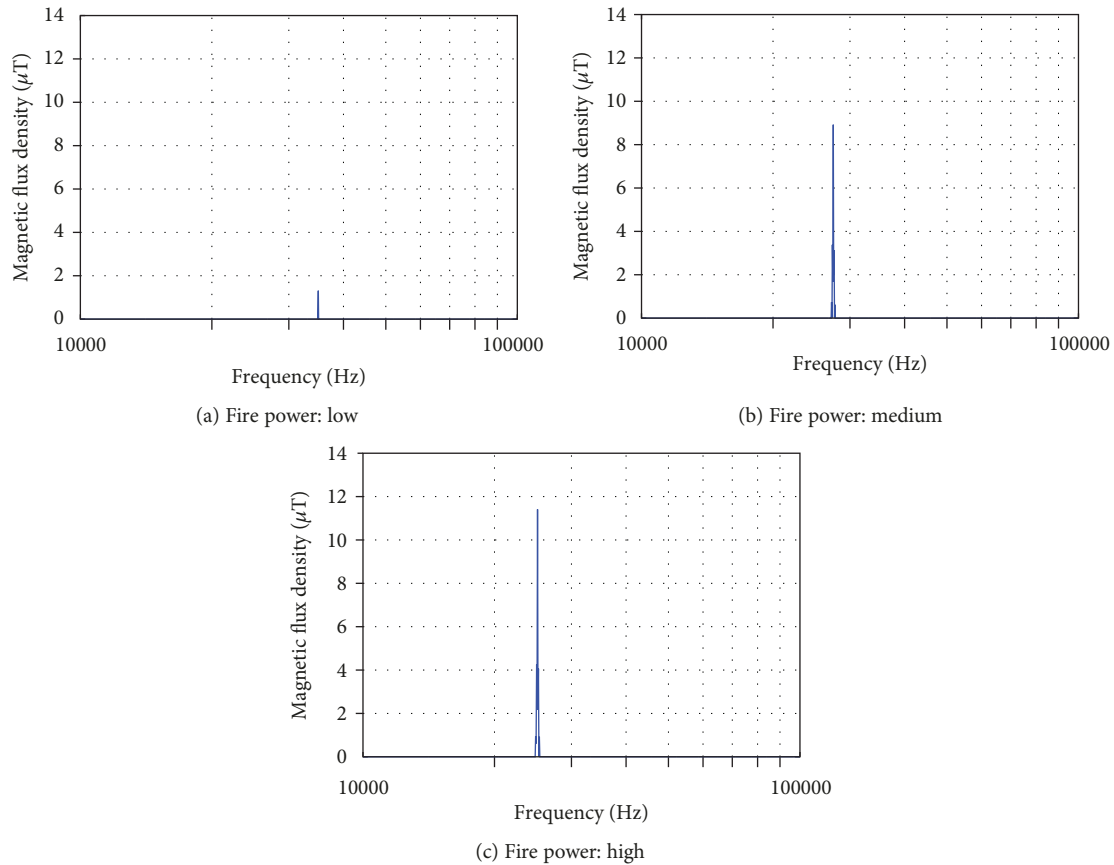


FIGURE 11: Change of magnetic flux density and operating frequency depending on fire power.

of negative width (in front of the cooking heater where a cook is expected to stand). The maximum magnetic flux density is less than  $12 \mu\text{T}$ . In order to show distribution of magnetic flux density clearly, in Figures 8 and 9, a red mark is allocated to  $12 \mu\text{T}$  and the gradation display is used depending on magnetic flux density. In Figures 7–9, the distribution of the magnetic flux density around the IH cooking heater can be easily recognized visually; the value is not high in the cooking space.

Magnetic field measurement is carried out at arbitrary spots in the present study, which are located discretely and randomly in space. Thus, the magnetic fields shown in Figures 7–Figure 9 are not consecutive (the same as in Figure 10).

**4.2. Visualization of the Distribution of the Magnetic Flux Density around IH Cooking Heater-2.** Another IH cooking heater (2.0 kW) is also targeted. This IH cooking heater was manufactured more than 10 years ago and is much older than IH cooking heater-1. A smaller pan is used to fit the coil size of the IH cooking heater, and measurement of magnetic flux density is carried out.

The three-dimensional distribution of the magnetic flux density around IH cooking heater-2 is shown in Figure 10. Magnetic flux density at 492 measurement points is indicated. In this figure, the solid-line circle means the position of the IH cooking heater and two dotted lines mean the upper and lower edges, respectively, of the pan.

According to Figure 10, high magnetic flux density is observed in some points, especially in the area close to the IH cooking heater's plate and the side of the pan. At several points, magnetic flux density exceeds  $100 \mu\text{T}$ . Though the magnetic flux density is high around the IH cooking heater, it is low in the cooking space.

This magnetic field sensor can measure both the magnetic flux density and its frequency components. The frequency spectrum of the magnetic field is available at any point and at any time once turning on the switch connected to the detector's body. This function is valuable especially in the cases when frequency components of magnetic field depend on location and/or time of measurement.

In general, the main operating frequency of the IH cooking heater is between 20 and 50 kHz. The developed magnetic sensor covers the frequency range. It is a potentially powerful tool to investigate characteristics of magnetic flux density during the period that an IH cooking heater starts to operate and reaches the constant fire power.

Figure 11 shows the change of the frequency spectrum in the range of 10 and 100 kHz, which is obtained at the point of the edge of table of the IH cooking heater. It is clearly confirmed that both the frequency component of magnetic flux density and its magnitude change depending on the level of fire power. This is the selling point of the proposed system, which will be especially useful for characterization of magnetic flux density generated by an invertered apparatus/appliance.



FIGURE 12: Visualization of the magnetic field of the area around the vacuum cleaner.

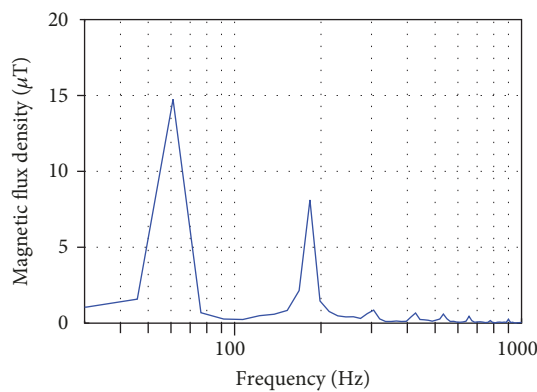


FIGURE 13: Frequency spectrum of the magnetic flux density measured at the top of the vacuum cleaner.

**4.3. Visualization of the Distribution of the Magnetic Flux Density around the Vacuum Cleaner.** When the industrial vacuum cleaner is operating with strong suction, the visualization of magnetic flux density around it is performed. The result is shown in Figure 12. This visualization system reveals that the magnetic flux density is strong around the top of the vacuum cleaner and the maximum value is  $17.4 \mu\text{T}$ . Furthermore, the frequency spectrum at the point is shown in Figure 13. According to this figure, it is clear that currents at 60 and 180 Hz are predominant frequencies in this vacuum cleaner.

## 5. Conclusions

The authors developed a high-performance magnetic field sensor. The frequency band of the sensor is from 30 Hz to 400 kHz; this sensor can calculate both the resultant magnetic flux density and its frequency components simultaneously. They are displayed on the LCD of the detector; measured results are stored in the USB memory inserted into the port

on the front of the detector. Raspberry Pi installed in this sensor realizes fast and reliable data transmission via Wi-Fi, visualization of measurement results in a short time, and reduction in cost.

Next, as the application of the magnetic field sensor, the visualization method with the AR technology was proposed. The AR technology is a technique that allows virtual imagery to be combined with the real world. As a core technology, the skeleton tracking function of Kinect is used. Based on this tracking function of Kinect, an inexpensive visualization system was also proposed.

Finally, several experiments were carried out and the distribution of the magnetic flux density was visualized. Moreover, the operating frequency was also identified in a short transient period when fire power of a household appliance changes. This developed magnetic field sensor and the visualization system are particularly expected to be applicable for the analysis and the evaluation of electrical equipment.

However, there are some problems in this system. In regard to the magnetic field sensor, the measurement interval is restricted by the speed of the processing unit of the Raspberry Pi. Acceleration of the processing is necessary to improve the performance of the visualization system. Concerning the visualization system, the skeleton tracking function does not operate correctly when an object exists between the hands holding the probe and the Kinect sensor. Predicting the position of the hand during the tracking function stops is a future work.

Furthermore, as shown in Figures 7–10, there are points where no measurement result is shown. In order to obtain continuous positional distribution of the magnetic field, the magnetic field has to be measured at many points close to each other. The alternative is to calculate the magnetic field at a point without the measured value by interpolation using the magnetic field at adjacent measuring points. This is also a future work.

## Data Availability

The data used to support the findings of this study are included within the article.

## Conflicts of Interest

The authors declare that they have no conflicts of interest.

## References

- [1] S. Noguchi, Y. Matsubayashi, H. Yamashita, and V. Cingoski, "A new interactive visualization system with force feedback device in 3-D electromagnetics," *IEEE Transactions on Magnetics*, vol. 40, no. 2, pp. 1382–1385, 2004.
- [2] S. Matsutomo, K. Mitsufuji, Y. Hiasa, and S. Noguchi, "Real time simulation method of magnetic field for visualization system with augmented reality technology," *IEEE Transactions on Magnetics*, vol. 49, no. 5, pp. 1665–1668, 2013.
- [3] J. Lu, "High performance computation and interactive visualization of electromagnetics for engineering education programs," *IEEE Transactions on Magnetics*, vol. 48, no. 2, pp. 299–302, 2012.

- [4] M. Bullo, F. Dughiero, and E. Sieni, "Analysis of stray EM fields generated by induction cooktops," *IEEE Electromagnetic Compatibility Magazine*, vol. 2, no. 2, pp. 49–58, 2013.
- [5] Association for Electric Home Appliances, "Measurement of electromagnetic field generated by household appliances (10Hz-400kHz)," 2013, <https://www.aeha.or.jp/safety/emwave.html>.
- [6] M. Iida, Y. Koji, C. Ohkubo, Y. Mizuno, and K. Isaka, *Evaluation of Magnetic Fields Generated by Induction Hob under Assumed Actual Usage Conditions*, PA-101, BioEM, Asilomar, 2015.
- [7] I. Magne, F. Audran, E. Mayaudon, D. Clement, and F. Deschamps, "50Hz electric and magnetic field measurements in high voltage substations," in *International Colloquium Power Frequency Electromagnetic Fields ELF EMF, Paper 20*, Sarajevo, 2009.
- [8] D. Clement, F. Deschamps, I. Magne, and M. Burceanu, "Inter-Laboratory 50 Hz EMF Measurement," in *BioEM*, pp.519-521, Davos, Switzerland, 2009.
- [9] K. Tanaka, Y. Mizuno, and K. Naito, "Measurement of power frequency electric and magnetic fields near power facilities in several countries," *IEEE Transactions on Power Delivery*, vol. 26, no. 3, pp. 1508–1513, 2011.
- [10] Y. Miyaji, M. Shimada, Y. Mizuno, and K. Naito, "Evaluation of magnetic field generated by power distribution equipment in accordance with IEC 62110," *IEEJ Transactions on Fundamentals and Materials*, vol. 135, no. 5, pp. 282–286, 2015.
- [11] K. Isaka, N. Hayashi, Y. Yokoi, and M. Okamoto, "Characteristics of ground-level electric and magnetic fields generated by ac power transmission lines," *International Symposium on Electromagnetic Compatibility*, vol. 2, pp. 511–514, 1989.
- [12] S. E. Pandarakone and Y. Mizuno, "Advanced visualization system of magnetic field distribution using wireless magnetic sensor module and skeleton tracking Kinect," *IEEJ Transactions on Fundamentals and Materials*, vol. 137, no. 1, pp. 46–51, 2017.
- [13] "Magnetic Field Hitester," [https://www.hioki.com/en/products/detail/?product\\_key=5582](https://www.hioki.com/en/products/detail/?product_key=5582).
- [14] "ELT-400, Measuring device for evaluating safety in magnetic fields(1Hz-400kHz)," <https://www.narda-sts.us/page.php?ID=10&Z=Low+Frequency+Meters>.
- [15] <https://www.raspberrypi.org>.
- [16] "Kinect for Windows," <https://developer.microsoft.com/en-us/windows/kinect>.
- [17] H. Miyajima and M. Yamamoto, "Personal identification based on skeletal movement using Kinect," *The Journal of The Institute of Image Information and Television Engineers*, vol. 67, no. 11, pp. J417–J420, 2013.
- [18] I. Iimura, Y. Imamura, Y. Kiridoshi, Y. Moriyama, and S. Nakayama, "Self-organizing maps-based Japanese flag signaling recognition by using Kinect," *IEEJ Transactions on Electronics, Information and Systems*, vol. 135, no. 1, pp. 138–139, 2015.



**Hindawi**

Submit your manuscripts at  
[www.hindawi.com](http://www.hindawi.com)

